Free Radical Mediated X-Ray Damage of Model Membranes

Anchi Cheng and Martin Caffrey
Department of Chemistry, The Ohio State University, Columbus, Ohio 43210 USA

ABSTRACT The damaging effects of synchrotron-derived x rays on aqueous phospholipid dispersions have been evaluated. The effect of degree of lipid hydration, phospholipid chemical structure, mesophase identity, aqueous medium composition, and incident flux on the severity and progress of damage was quantified using time-resolved x-ray diffraction and chromatographic analysis of damage products. Electron spin resonance measurements of spin-trapped intermediates generated during irradiation suggest a free radical-mediated process. Surprisingly, radiation damage effects revealed by x-ray diffraction were imperceptible when the lamellar phases were prepared under water-stressed conditions, despite the fact that x-ray-induced chemical breakdown of the lipid occurred regardless of hydration level. Of the fully hydrated lipid systems studied, saturated diacyl-phosphatidylcholines were most sensitive to radiation damage compared to the ester- and ether-linked phosphatidylethanolamines and the ether-linked phosphatidylcholines. The inclusion of buffers or inorganic salts in the dispersing medium had only a minor effect in reducing damage development. A small inverse dose-rate effect was found when the x-ray beam intensity was changed 15-fold. These results contribute to our understanding of the mechanism of radiation damage, to our appreciation of the importance of monitoring both structure and composition when evaluating biomaterials radiation sensitivity, and to the development of strategies for eliminating or reducing the severity of damage due to an increasingly important source of x rays, synchrotron radiation. Because damage is shown to be free radical mediated, these results have an important bearing on age-related accumulation of free radicals in cells and how these might compromise membrane integrity, culminating in cell death.

INTRODUCTION

Third-generation synchrotron x-ray sources were designed for enhanced optical brightness and to meet the growing global demand for synchrotron-derived x rays. From the perspective of structural biology research, synchrotron radiation has proved to be a boon in several areas. These include structure and kinetics studies of membranes and membrane components, muscle, biologically relevant thin films, and supramolecular and macromolecular crystallography. Despite the merits of synchrotron radiation, an important question remains to be answered as we anticipate the availability of even brighter sources. Simply put, the question is, can we use the delivered flux before the sample succumbs to radiation damage? By and large, the crystallographers will respond to increased flux and the prospect of radiation damage by resorting primarily to proven cryotechniques (Helliwell, 1984). Unfortunately, this is not a viable option for those involved in studies of kinetics and the mechanism of structural transformations in mesophases, membranes, muscle, etc. Radiation damage looms over these areas. It is imperative therefore that we set about the task of gaining an understanding of this unwanted process with a view to devising strategies and protocols that avoid the problem completely or that minimize the effects of damage. This report describes the results of one such study aimed at deciphering the mechanism of damage occurring in lipid membranes during the course of exposure to synchrotron-derived x rays.

Damage by x rays and other forms of ionizing radiation of organic materials is believed to proceed through the generation and chain reactions of free radicals (Swartz and Swartz, 1983). When an amphiphilic or hydrophilic organic substance dispersed in water is exposed to ionizing radiation, free radicals can be generated directly, as a result of the substance itself absorbing the ionizing radiation, or indirectly, through reactions with reactive free radicals arising from water radiolysis (Stark, 1991). Less severe, and often reversible "damage" can also arise as a result of sample heating by the incident beam. In the case of amphiphiles, such as the lipids used in the current study, the structural changes observed as a result of radiation damage depend on the chemical nature of the amphiphile and the products of radiation damage as well as the physical constraints imposed by sample composition, water content in particular.

We became painfully aware of the radiation damage issue several years ago upon realizing that x-ray damage had compromised some of our lipid diffraction measurements made at a synchrotron source (Caffrey, 1985; Caffrey and Bilderback, 1984; Cheng et al., 1993). To better understand this destructive process, a series of measurements were performed to investigate in as systematic a way as possible the manner in which x rays interact with such materials. We used x-ray diffraction to identify mesophases and to characterize them structurally during the damaging process. Thin-layer chromatography (TLC) was used to monitor x-radiation-induced changes in chemical composition. In

Received for publication 10 July 1995 and in final form 9 February 1996.

Dedicated to Professor George A. Jeffery on the occassion of his 80th birthday.

Address reprint requests to Dr. Martin Caffrey, Department of Chemistry, Ohio State University, 120 W. 18th Ave., Columbus, OH 43210. Tel.: 614-292-8437; Fax: 614-292-1532; E-mail: caffrey+@osu.edu.

0006-3495/96/05/2212/11 $2.00

addition, electron spin resonance (ESR) spectroscopy was performed to evaluate the proposed radical-mediated damage mechanism. In this report, we describe the results of these measurements performed to evaluate quantitatively the nature of x-radiation-induced damage as affected by lipid headgroup identity, type of linkage between lipid headgroup and hydrocarbon chain, chain length and unsaturation, hydration, aqueous medium composition, beam intensity, and temperature.

MATERIALS AND METHODS

Materials

All ester-linked phospholipids used in this study were obtained from Avanti Polar Lipids (Birmingham, AL). 1,2-Dihexadecyl-*sn*-glycero-3-phosphocholine was from Serdary Research Laboratory (London, ON) and 1,2-dihexadecyl-*sn*-glycero-3-phosphoethanolamine (DHPE) was either from Serdary or from Fluka Chemical (Hauppage, NY). Palmitic acid and dipalmitin were from Nu Chek Prep. (Elysian, MN), and monomyristin was from Fisher Scientific (Pittsburgh). Lipid purity was checked by TLC as described below, and lipids were shown to be >99% pure. 2-Methyl-2-nitrosopropane (MNP) was obtained from Sigma Chemical Co. Water used in sample preparation was obtained from a Milli-Q purification system (Millipore Corp., Bedford, MA). Solvents used in the ESR measurements were of spectroscopic grade. Other chemicals were of reagent grade.

Sample preparation

The procedures used for mechanical mixing and for lipid and aqueous medium concentration determination of the final dispersion have been described previously (Briggs and Caffrey, 1994). The lipid dispersion was injected into 1-mm-O.D. quartz capillaries (Supper) carefully selected to be uniform in O.D. to ±0.05 mm. The concentration of water in so-called excess water samples was more than or equal to 50% (w/w). Temperature control was better than ±0.1°C and was effected using a thermoelectric temperature controller (Briggs and Caffrey, 1994).

X-ray sources

X-ray damage was effected and diffraction measurements were made with wiggler-enhanced synchrotron radiation in the A1 and the F1 stations at the Cornell High-Energy Synchrotron Source (CHESS) and with bending magnet x rays in the X9B station at the National Synchrotron Light Source (NSLS). Both x-ray sources and optics at these facilities have been described previously (Briggs and Caffrey, 1994). The corresponding flux in the A1 and F1 stations at CHESS through a 0.3-mm collimator (Supper) and in the X9B station (measured beam size at the sample = 0.5–0.7 × 2.3–3.0 mm^2) at NSLS were ~2×10^{10}, 2×10^{11}, and 2×10^{11} photons/s, respectively. All data presented in this report were collected in the A1 station at CHESS unless otherwise noted.

Thin-layer chromatography

Thin-layer chromatography was used regularly as a check on lipid purity before and after each experimental manipulation and for purposes of identifying chemical breakdown products in radiation damage studies.

The thin-layer plates (Adsorbosil-Plus Prekotes, no. 16385; Alltech, Deerfield, IL) were pre-run once in chloroform:methanol (10:1 v/v) and were activated on a hot plate (~240°C) immediately before use. Three polar solvent systems (chloroform:methanol:water (65:25:4 v/v/v), chloroform:methanol ammonium hydroxide (28% v) (65:25:5 v/v/v), and chloroform:methanol:acetic acid:acetone:water (10:2:2:4:1 v/v/v/v/v) (Caffrey and Feigenson, 1981) and petroleum ether:diethyl ether:acetic acid (70:30:0.5 v/v/v) were used. The lipid samples, in the form of a dry powder or an aqueous dispersion, were dissolved in chloroform:methanol (2:1 v/v). Vacuum drying of the aqueous dispersion was not performed.

Quantities of lipid in chloroform:methanol (2:1 v/v) were loaded onto TLC plates, giving spot sizes ranging from 0.5 to 100 μg lipid. The plates were developed in one of the above solvent systems and were visualized by charring on a hot plate (240°C) after spraying with Zinzadze reagent (Dittmer and Lester, 1964). Sample purity was determined quantitatively by comparing visually the intensities of the 0.5- and 1-μg spots to the impurity level in lanes corresponding to the 100-μg sample.

Identification of the breakdown products was made by comparing the retention factor of standards (lysophosphatidylcholine (lysoPC), monoacylglycerol, diacylglycerol, and fatty acid) with that of the breakdown products in the sample lane. In all cases, standards and samples were loaded on the same plate to facilitate direct comparisons.

In all measurements where x-ray diffraction was used to monitor radiation damage, the minimum sample volume used was 5 μl. Using a 0.3-mm collimator and a 1-mm-diameter sample capillary at CHESS, the irradiated volume was less than 1.4% of the total sample volume. Breakdown product represents only 0.7% of the total sample if 50% of the lipid succumbs to radiation damage. Accordingly, chromatographic analysis of samples representing the entire sample after the exposure is unlikely to be sensitive to highly localized x-ray damage. It is important therefore to recognize that the apparent absence of breakdown products as judged by analysis of the type just described after an x-ray measurement does not guarantee that radiation damage has not occurred as discussed previously (Caffrey, 1984). To ensure that the irradiated region represents a large fraction of total sample volume, thereby enhancing the sensitivity of the analysis, a 1-μl lipid dispersion contained in a 2-mm-diameter capillary was exposed to the uncollimated x-ray beam. We estimate that ~55% of the total sample volume is exposed to x rays under these conditions. At the beginning and end of the exposure, x-ray diffraction patterns were recorded from the same sample, with the collimator in place to monitor changes in diffraction behavior induced by the irradiation process.

Spin trapping measurements

The spin trap used in this study was MNP. Because MNP is light sensitive, preparation of a 0.01 M MNP aqueous solution at 40°C (Makino et al., 1981), mechanical mixing of the lipid sample with the MNP solution, x-irradiation, and the subsequent ESR measurements were performed under subdued light. ESR recordings were made using 0.15 ml of sample containing 1,2-dimyristoyl-*sn*-glycero-3-phosphocholine (DMPC)/0.01 M MNP aqueous solution/chloroform:methanol (2:1 v/v) in the ratio 36 mg/36 μl/500 μl. Spectra were recorded at room temperature in a flat quartz cell (WG-813; Wilmad Glass, Buena, NJ) using a Bruker ER-300 spectrometer (Brookfield Center, CT).

X-ray diffraction and analysis

X-ray diffraction patterns were obtained during continuous sample irradiation using a home-built, multi-frame camera with a computer-controlled shutter downstream of the sample. Image plates were used for recording data whenever possible because they offer high sensitivity, good linearity, and a large dynamic range. Image plate data were processed as described previously with the following modifications (Cheng et al., 1996). Powder diffraction patterns were radially averaged over a 5° to 7° arc centered on the vertical axis to produce intensity-scattering vector (I-s) plots. Some diffraction patterns were recorded on x-ray-sensitive film, in which case one-dimensional densitometric scans were made using a laser scanning densitometer (model SLR-2D/1/D; Biomed, Fullerton, CA). The processed data obtained from film is noisier than that from image plates. However, the detector type did not have an impact on the conclusions of this study.

A quantitative evaluation of x-ray damage as judged by changes in low-angle diffraction with accumulated dose has proved to be a nontrivial

undertaking. What we find is that changes take place simultaneously in both the sharp Bragg peaks and in the level of diffuse scatter between and beneath these peaks. For purposes of quantifying radiation damage, therefore, we introduce what is called a normalized order index, $\tilde{A}_{hkl}(i)$, as a measure of the effects of damage. $\tilde{A}_{hkl}(i)$ is defined with reference to the second-order lamellar reflection (hkl = 002, or the 02 reflection in the case of the inverted hexagonal (H_{II}) phase) and to diffuse scatter in its immediate vicinity. $\tilde{A}_{hkl}(i)$ varies from 1 in the absence of radiation damage to negative values in severely damaged samples. The index i in $\tilde{A}_{hkl}(i)$ refers to the "frame or diffraction pattern number," recorded during the course of the x-ray damage experiment. Thus, i = 1 represents the zero-time exposure recorded at the start of the experiment. The latter is used as a reference benchmark for determining $\tilde{A}_{hkl}(i)$ as described below.

Shown in Fig. 1 are low-angle I-s scans recorded at the beginning (i = 1, Fig. 1 A) and at the end (Fig. 1 B, in this case i = 15) of an x-ray damage experiment. These two profiles will be used to illustrate how $\tilde{A}_{hkl}(i)$ is calculated, as follows. To begin with, the intensity level of $I_b(1)$ between the (001) and (002) reflections is taken as the average I value between s_1 and s_2 in Fig. 1 A. s_1 and s_2 are chosen to define the flattest part of the I-s profile between the (001) and (002) reflections in the zero-time exposure. A horizontal line is then drawn between s_1 and s_2 at the $I_b(1)$ level and is extended in the high-s direction until it crosses the I-s profile on the high-s side of the (002) peak at s_3 in Fig. 1 A. The next step is to measure the area of the (002) peak above $I_b(1)$, which is identified as $A_{002}(1)$. This same procedure is repeated for the series of frames recorded during the course of the radiation damage experiment, holding s_1, s_2, and s_3 fixed throughout the analysis. As is shown in Fig. 1 B, where i = 15 and the sample is severely damaged, $I_b(15) > I_b(1)$ and $I_p(15)$, the consequence of which is that $A_{002}(15)$ is a negative quantity. During the course of a radiation damage experiment, incident beam intensity, $I_o(i)$, decreases. To correct for this effect, $A_{hkl}(i)$ is normalized by dividing each value by the corresponding $I_o(i)$. Because the normalized data can be noisy, we felt it important not to weight too heavily the i = 1 datum in the analysis. To this end, the $A_{hkl}(i)/I_o(i)$ data are plotted as a function of accumulated dose and fitted with a smooth, monotonic function of the form $y = a\exp(-(x/b)^2) + c$, where y represents $A_{hkl}(i)/I_o(i)$, x is the accumulated dose, and a, b, and c are fitted parameters. The fitted value, referred to as $A_{hkl}(1)'/I_o(1)'$, is obtained by setting x = 0 in the above equation and is used in calculating the required normalized order index, $\tilde{A}_{hkl}(i)$, as

$$\tilde{A}_{hkl}(i) = [A_{hkl}(i)/I_o(i)]/[A_{hkl}(1)'/I_o(1)']. \quad (1)$$

It is this quantity that is plotted as a function of accumulated dose under Results. $\tilde{A}_{hkl}(i)$ is a measure of ordered structure associated with the hkl reflection scaled to its best-fitting initial value. Notice that negative values of $\tilde{A}_{hkl}(i)$ can arise when the diffuse scattering level rises above the Bragg peak, as applies in the example shown in Fig. 1 B for a severely radiation-damaged sample.

The normalized order index above is introduced as a means of describing changes in low-angle diffraction behavior that accompany damage in as quantitative a manner as possible. Unfortunately, because radiation damage effects on mesophase structure are complex, neither the magnitude nor the sign of the normalized order index has direct physical meaning. However, the index does provide a means of describing the changing diffraction data simply and without the need for assumptions. There are three technical reasons that have prevented a more detailed analysis of the course of the structure changes accompanying radiation damage: 1) The I-s profile of the low-angle diffuse scatter changes during the course of x-irradiation. Accordingly, it was not possible to describe consistently throughout the exposure the diffuse scattering profile with a small number of parameters. 2) Careful peak profile analysis of data collected with highly collimated x-ray beams has been used to characterize lattice disorder in lyotropic mesophases (Blaurock, 1982; Wiener and White, 1991). The current measurements were performed with a simple slit arrangement incorporating relatively wide slits, and no attempt was made to procure a highly collimated x-ray beam. As a result, a detailed I-s profile analysis of the data with a view to identifying disorder type is not appropriate. 3) The majority of the data collected in this study were centered on the first two low-angle orders of diffraction, because this is where the most dramatic changes occur during damage and because higher order reflections are vanishingly weak in the fully hydrated lamellar liquid crystalline (L_α) phase of phosphatidylcholine (PC) samples. This compromises an analysis of the type noted above, where the widths of several Bragg reflections must be compared.

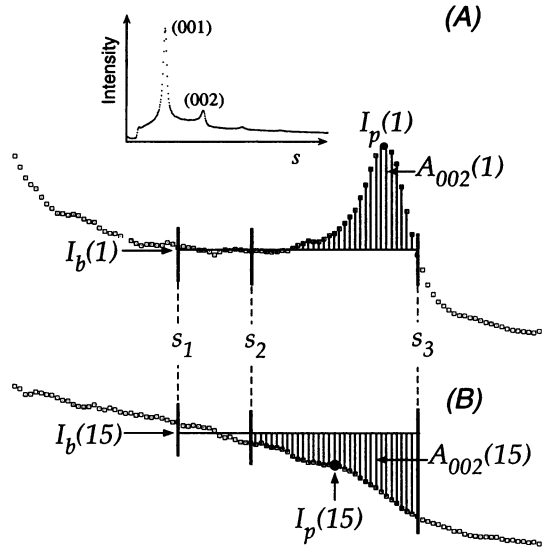

FIGURE 1 Quantitative evaluation of x-radiation-induced changes in low-angle x-ray diffraction from hydrated DPPC recorded on an image plate detector. Shown as an inset in A is the low-angle diffraction I-s profile from DPPC in the $L_{\beta'}$ phase at 46% (w/w) water and 30°C, which includes the (001) (at 61 Å) and (002) (30 Å) lamellar reflections as indicated. This diffraction pattern was recorded using a sample that had not been previously exposed to x rays and represents a zero time exposure (as in frame 1, Fig. 3). An expanded view of the (002) reflection is shown in A. After extensive irradiation, the (002) reflection almost completely disappears and is buried in diffuse scatter, as shown in B (as in frame 15, Fig. 3). Scattering background defining and integration regions are based on zero-time exposure diffraction patterns as shown in A. The area of integration is measured relative to the level ($I_b(i)$) and can be a positive value, as in A, or a negative value, as in B, depending on the severity of radiation damage. See text for details.

Calculation of accumulated radiation dose

The procedure used to calculate the accumulated radiation dose has been described previously (Caffrey, 1984). Briefly, the incident x-ray flux, i.e., the total number of x-ray photons entering the lipid sample per unit time, was measured with nitrogen-filled (CHESS) or argon-filled (NSLS) ionization chambers with path lengths ranging from ¼ inch to 3¾ inch. The energy absorbed by the sample during the irradiation was calculated based on the following assumptions: 1) the x rays used were monochromatic, 2) the density of the lipid dispersion was 1 g·cm^{-3}, 3) the diameter of the x-ray capillary was 1 mm, 4) the x-ray intensity was uniformly distributed in the irradiated sample cross section, 5) the irradiated sample cross-sectional area was 0.3 × 0.3 × π/4 mm^2 at CHESS, where most of the experiments presented here were performed, and 6) the measurements at NSLS were made with beams having cross-sectional areas at the sample of 0.5 × 2.3 mm^2 for the dose rate comparison study and 0.7 × 3.0 mm^2 for the DMPC hydration series study. The mass absorption coefficients for the sample were calculated according to the elemental composition of the sample and their mass absorption coefficients (MacGillavry and Rieck, 1983). The accumulated radiation dose is presented in rads, where 1 rad

corresponds to the absorption of 10^{-2} J of ionizing radiation by 1 kg of material (1 rad = 0.01 Gy (gray) = 0.01 J/kg = 100 erg/g).

A cautionary note

The accumulated dose calculated as described above can well be used to compare the effects of radiation damage at different synchrotron sources and different times, provided flux intensity is uniform across the beam. In the course of this study, however, we noticed that the same calculated accumulated dose did not always produce equivalent damage effects as determined by diffraction. As a result, it was deemed necessary to limit comparisons of radiation damage effects to a single experimental period. The reason for the inconsistency is not known. One possibility is that the incident x-ray beam is not uniform, which leads to an incorrect calculation of accumulated dose. Accordingly, we emphasize the need to include careful beam profile analysis in all future studies of radiation damage effects.

RESULTS AND DISCUSSION

Free radical-mediated x-ray damage

Ionizing radiation damage of organic material in an aqueous medium is believed to proceed through the generation of free radicals (Swartz and Swartz, 1983). Such radicals are short-lived and, therefore, are hard to detect directly in the absence of an in situ measurement. This difficulty can be overcome by implementing a spin-trapping technique where a more stable, long-lived nitroxide derivative (spin adduct) is produced from the transient radical (spin) (Evans, 1979). The use of spin traps was implemented in the present study of x-radiation damage to DMPC.

Fig. 2 presents a comparison of the ESR spectrum of an aqueous MNP spin trap solution x-irradiated in the presence and absence of DMPC. No evidence for radical production was found in the MNP solution or the lipid/MNP aqueous dispersion that had not been exposed to x rays. The ESR signal of the lipid-containing sample is significantly stronger than that of the lipid-free MNP solution measured under identical conditions. The spectral profile of the lipid sample is asymmetric, suggesting that more than one kind of spin adduct is present in the solution containing the irradiated lipid. One of these is probably the free radical generated by the dispersing MNP solution itself. The others presumably derive from the products of lipid x-ray damage. An attempt was made to extract into benzene the spin adducts so generated. The adducts did not partition significantly into this apolar solvent, suggesting that the trapped radicals are hydrophilic and may be either charged or polar.

FIGURE 2 ESR spectrum of an aqueous MNP solution after x-irradiation in the presence (——) and absence (– – –) of DMPC. Hyperfine splitting constants are 15.2 and 16.0 G, respectively. The total dose in each case was 15 Mrad (61% absorption assumed), and exposures were made at a dose rate of 14 krad/s. Radicals observed are stable for at least a week at 4°C. The ESR spectra were obtained at room temperature with the following ESR spectrometer settings: microwave power, 20 mW; field, 3465 ± 50 G; conversion, 163.84 ms; time constant, 655 ms; sweep time, 167.772 s; modulation frequency, 100.000 kHz; modulation amplitude, 1.013 G; receiver gain, 5.00×10^5; number of scans, 1.

Radiation damage as monitored by x-ray diffraction

Diffraction techniques are widely used to monitor the progress of radiation damage in mesophases because they are sensitive to changes in mesophase structure. Thus, saturated PCs have been studied in this way upon exposure to β particles (Hui, 1980), x rays (Caffrey, 1984), and γ-rays (Katsaras et al., 1986; Mariani and Rustichelli, 1989, and references therein). Diffraction intensity variation has also been used to examine degradation involving single crystals (Stout and Jensen, 1989, pp. 183–184).

We have observed two types of damage-induced diffraction pattern changes in hydrated lipids. The first, hereafter referred to as Type I damage, takes the form of a disordering of structure coupled to a lamellar swelling process. Type I damage is evidenced by a decrease in Bragg intensity and increases in diffraction peak width, in diffuse scattering, and in lamellar repeat. Damage of the second type (Type II) involves the formation of a nonbilayer phase in a lamellar environment evidenced by the emergence of hexagonal phase reflections in a lamellar phase background and a loss of intensity associated with the lamellar phase (Cheng et al., 1993). In Type II damage, diffuse scatter and diffraction peak profiles do not change significantly during the course of radiation damage. The current study focuses on damage of the first type.

The consequences of x-radiation damage to fully hydrated 1,2-dipalmitoyl-*sn*-glycero-3-phosphocholine (DPPC) in the lamellar gel phase with tilted chains ($L_{\beta'}$ phase) at 25°C is shown in Fig. 3. This is typical of Type I damage, where disordering of the mesophase structure prevails. In the early stages of the exposure, and presumably before damage was significant (frame 1, t = 0 min in Fig. 3), lamellar and chain-packing diffraction peaks were sharp and strong. With continued exposure, all Bragg reflections in the low-angle and wide-angle region weaken and diffuse scattering intensifies. Specifically, in the low-angle region, the (002) reflection becomes buried in the diffuse scatter after ~6 min (6.5 Mrad), as shown in Fig. 3 (frame 10). Diffuse scattering dominated the pattern in the latter part of the exposure period. Accompanying the decay in the lamellar diffracted intensity is an increase in the lamellar repeat size at the rate of ~0.25 Å/Mrad. The damaging effects observed in the low-angle diffraction behavior of fully hydrated DPPC in the L_α phase are qualitatively similar to those recorded for the $L_{\beta'}$ phase of this same system.

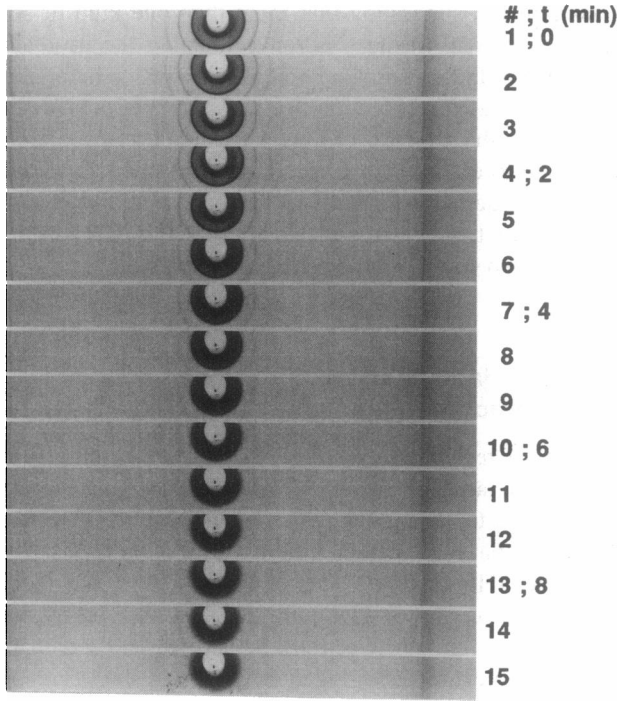

FIGURE 3 X-ray-induced changes in the mesophase structure of fully hydrated DPPC. Low-angle diffraction from the lipid recorded on x-ray-sensitive film is shown as a series of consecutive x-ray photographs (exposure time, 30 s) recorded in intervals of 40 s during continuous x-irradiation of the sample for 10 min. Measurements were performed at 25°C using focused monochromatic x rays at 1.56 Å (8 keV) in the A1 station at CHESS. The incident flux on the sample was 1.7×10^{10} photons/s (18 krad/s). The sample-to-detector distance was 11 cm, and sequential patterns were recorded in 1.0-cm-wide strips on a 12.5 cm × 17.5 cm Kodak DEF-5 x-ray sensitive film. Frame number and elapsed time are indicated.

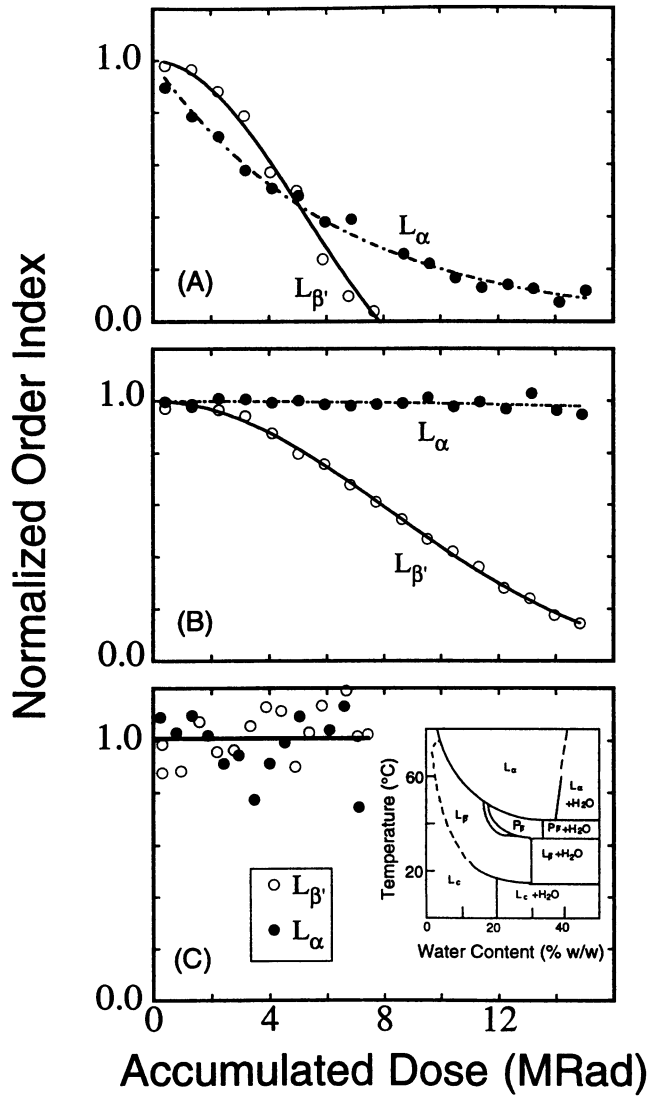

FIGURE 4 Effect of hydration level on x-ray-induced changes in low-angle diffraction behavior of the L_α (65°C) and $L_{\beta'}$ (30°C) phases of DPPC. (*A*) 46% (w/w) water; (*B*) 34% (w/w) water; (*C*) 14% (w/w) water. Lines are drawn simply to guide the eye. A schematic temperature-composition phase diagram for DPPC/water is shown as an inset in *C* (Janiak et al., 1976; as presented in Cevc and Marsh, 1987).

As might be expected, however, little, if any, change in the diffuse wide-angle scattering from the L_α phase was detected.

Effects of hydration

Our measurements show that radiation damage effects as monitored by x-ray diffraction are particularly sensitive to lipid hydration. We observed that the diffraction profile of fully hydrated saturated PCs changed quite readily upon irradiation in both the $L_{\beta'}$ and the L_α phases. In distinct contrast, when the lipid was maintained under conditions where it is less than fully hydrated, the low- and wide-angle diffracted intensity and the d-spacings of the low-angle diffraction were no longer sensitive to x-radiation exposure in the range studied. We demonstrated this dramatic hydration-dependent behavior by exploiting the differences in maximum hydration level of the $L_{\beta'}$ and the L_α phases in the DPPC/water system (Fig. 4).

The hydration limit of the $L_{\beta'}$ and L_α phases formed by DPPC is ~40% and 30% (w/w) water, respectively (Janiak et al., 1979) (Fig. 4 *C*). Accordingly, a DPPC sample with >40% (w/w) water is fully hydrated, regardless of mesophase type in the 0 to 70°C range. In this excess water regime, we found that our measure of x-radiation damage, the so-called normalized order index of mesophase structure, decreases significantly with accumulated x-ray dose in both the $L_{\beta'}$ and L_α phases (Fig. 4 *A*). In the hydration range between 30% and 40% (w/w) water, the lipid is water-stressed in the L_α phase but not in the $L_{\beta'}$ phase. Such a sample showed little x-ray-induced Bragg diffraction intensity decay in the water-stressed L_α phase at 65°C (Fig. 4 *B*). In contrast, the diffracted intensity from the $L_{\beta'}$ phase at 30°C, where the sample is in equilibrium with excess water, was strongly influenced by x-irradiation (Fig. 4 *B*). At hydration levels below 30% (w/w) water, little Bragg diffraction intensity decay was found in the L_α phase at 65°C

or in the $L_{\beta'}$ phase at 30°C, where the lipid was water-stressed in both mesophases (Fig. 4 *C*). Similar results were obtained with DMPC at hydration levels between 30% and 40% (w/w) (Fig. 5 *B*). However, fully hydrated DMPC did show only a slight loss in Bragg diffraction intensity in the L_α phase, where a pronounced loss was seen under comparable conditions with DPPC (compare Figs. 4 *A* and 5 *A*).

We have shown that the responsivity of PCs to x-ray damage as judged by x-ray diffraction is sensitive to sample hydration level. The possibility exists, however, that the sample is succumbing to the same degree of radiation damage regardless of hydration level, but that the mesophase structural sensitivity and consequences differ, depending on the water content of the sample. In this context, therefore, an obvious question to ask is whether chemical breakdown is occurring under both fully hydrated and water-stressed conditions, regardless of the marked difference in the observed diffraction-based change in order index. To address this question, we performed TLC analysis on DMPC and DPPC dispersions containing between 30% and 40% (w/w) water in different mesophase types with equivalent accumulated dose levels (Fig. 6). Despite the very different damage effects seen by x-ray diffraction, common breakdown products such as lysoPC and free fatty acid were found in samples irradiated in either the water-stressed L_α phase or the fully hydrated $L_{\beta'}$ phase (Fig. 6). The data shown in Fig. 6 relate to DMPC. Similar results were obtained with DPPC.

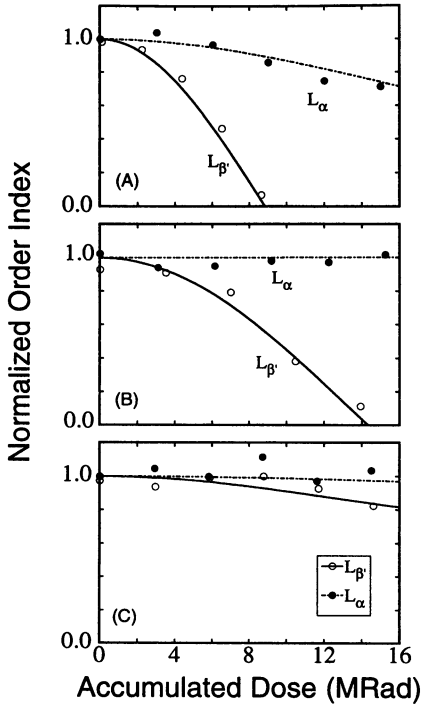

FIGURE 5 Effect of hydration level on the x-ray-induced changes in low-angle diffraction behavior of the L_α (29°C) and $L_{\beta'}$ (10°C) phases of DMPC. (*A*) 47% (w/w) water; (*B*) 36% (w/w) water; (*C*) 20% (w/w) water. Lines are drawn simply to guide the eye. Data collected in the X9B station at NSLS. Similar results were obtained for this system at CHESS.

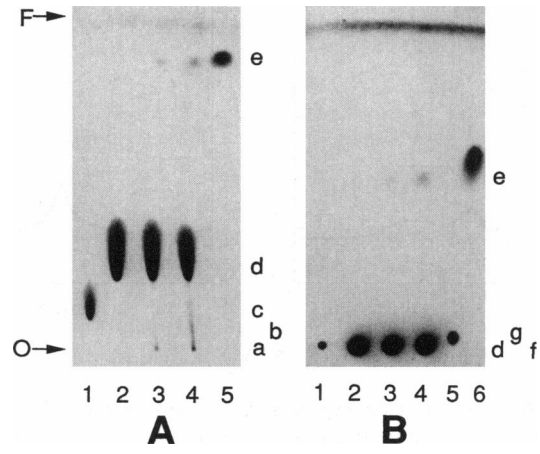

FIGURE 6 Thin-layer chromatograms of x-irradiated (*lanes 3* and *4*) and control (nonirradiated, *lane 2*) samples of DMPC at 34% (w/w) water to reveal chemical changes induced by continuous exposure to x rays. The irradiated sample had been in the uncollimated 13.6 keV x-ray beam on the F1 station at CHESS for 5.6 min (~50 Mrad) at 29°C (in the water stressed L_α phase, *lane 3*) or 10°C (in the fully hydrated $L_{\beta'}$ phase, *lane 4*). Both samples show significant chemical breakdown. The extent of the radiation damage as monitored by x-ray diffraction was recorded after the exposure. The solvent system was chloroform:methanol:water (65:25:4 v/v/v) (*A*) and petroleum ether:diethyl ether:acetic acid (70:30:0.5 v/v/v) (*B*). See text for details. The origin (O) and solvent front (F) are identified. The lipid standards used were 1-palmitoyl-*sn*-glycero-3-phosphocholine, *A1*; palmitic acid, *A5*, *B6*; dipalmitin, *B1*; and monomyristin, *B5*. Spots on the chromatogram are identified as follows: *a*, *b*: phosphate positive, unidentified; *c*: phosphate positive, lysoPC; *d*: DMPC; *e*: phosphate negative, fatty acid; *f*: phosphate negative, diacylglycerol; *g*: phosphate negative, monoacylglycerol.

Because irreversible chemical breakdown occurs under both fully hydrated and water-stressed conditions, we surmised that the hydration-dependent difference observed in the order index change with accumulated dose is a result of the different physical microenvironments that prevail in such systems. To test this hypothesis, the following experiment was performed. DMPC, at 34% (w/w) water and 29°C in the water-stressed L_α phase, was x-irradiated to an accumulated dose level sufficiently large to induce a significant reduction in the order index parameter under excess water conditions. Because this sample at this temperature is water-stressed, no reduction in order index parameter is observed and the low-angle diffraction peaks are characteristically sharp (Fig. 7). After the irradiation, temperature was lowered to position the sample in the region where the $L_{\beta'}$ phase normally appears. At 34% (w/w) water and 10°C, the $L_{\beta'}$ phase is in equilibrium with an excess water phase. The expectation was that the latter should allow the damage products accumulated during exposure in the L_α phase to elicit their effects in this new-found condition where excess water is available. This is precisely what was found experimentally. As can be seen in Fig. 7, the sample, previously exposed in the water-stressed L_α phase and subsequently placed in the $L_{\beta'}$ phase with excess water simply by lowering temperature, shows diffraction behavior analogous to that seen in a heavily damaged sample of fully hydrated $L_{\beta'}$

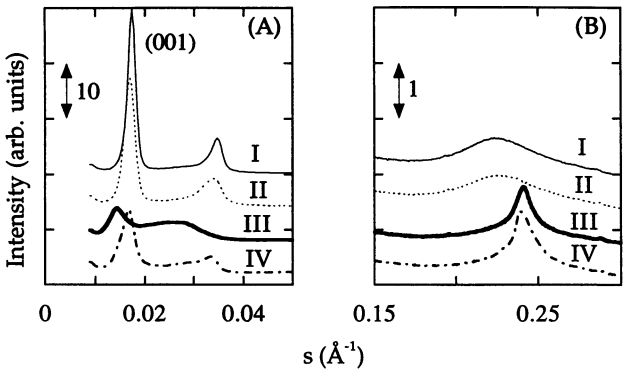

FIGURE 7 A test of the hypothesis that x-radiation damage effects, as monitored by x-ray diffraction, require the presence of an excess water phase for expression. Low-angle (*A*) and wide-angle (*B*) diffraction patterns from DMPC in the L_α phase at 34% (w/w) water (representing the water-stressed condition) were recorded and 29°C with 0 Mrad (I) and 50 Mrad (II) of x-ray exposure. Very little change in the diffraction pattern is apparent under these conditions of water stress. The sample giving rise to pattern II was subsequently cooled to 10°C, where the $L_{\beta'}$ phase forms under normal conditions and the diffraction pattern (III) was recorded once again by irradiating in the same spot used to collect data for pattern II. Pattern III is what is expected for extensive radiation damaged $L_{\beta'}$ phase in excess water. At 10°C and overall sample composition of 34% (w/w) water, this sample is expected to be under conditions of excess water. The pattern shown in IV was recorded by translating the capillary by 0.6 mm in the direction perpendicular to the x-ray beam to expose a fresh region of the sample that had not previously been x-irradiated. Pattern IV is typical of $L_{\beta'}$ phase in equilibrium with excess water.

phase. These data show convincingly that x-ray damage occurs and that damage products accumulate in this system during x-ray exposure, regardless of lipid hydration status, but that neither is apparent as a change in diffraction behavior unless an excess water phase is present.

The exact role played by the excess water phase in allowing radiation damage to express itself in the form of a reduced order index parameter is not known. However, in the course of the damaging process, free fatty acid and lyso lipid are produced, both of which can induce structural

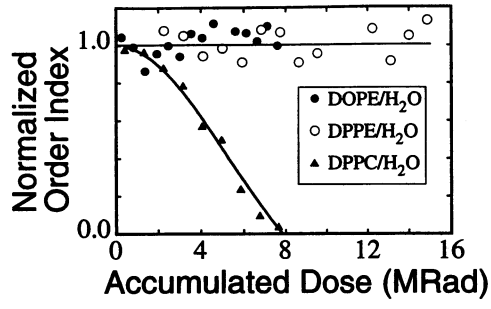

FIGURE 8 Sensitivity of phospholipid mesophases to x-radiation damage at 8 keV as monitored by changes in the low-angle diffraction of dispersions prepared at 50% (w/w) water. Relevant experimental conditions: DPPC, 65°C, L_α phase; DPPE, 1,2-dipalmitoyl-*sn*-glycero-3-phosphoethanolamine, 67°C, L_α phase; DOPE, 1,2-dioleoyl-*sn*-glycero-3-phosphoethanolamine, 30°C, H_{II} phase. Lines are drawn simply to guide the eye.

changes in a lamellar mesophase (Jansson et al., 1990; Katsaras et al., 1986). At low levels and under water-stressed conditions, these and other breakdown products accumulate within the existing lamellar architecture, and their effects on mesophase structure are miniscule. However, when an excess water phase is available, the presence of anionic free fatty acids at least should cause the lipid bilayers to separate, because of electrostatic repulsion, and the mesophase to imbibe water (Katsaras et al., 1986). Evidence for such an effect was found in the current study in that radiation damage was accompanied by an increase in the lamellar repeat. Lyso lipid, at sufficiently high concentrations, can give rise to a complete solubilization and disruption of the multilamellar structure. This would account for the loss in low-angle Bragg diffracted intensity associated with the lamellar reflections and for the appearance of diffuse scatter in this region.

Effects of lipid headgroup type, ether versus ester linkage, and mesophase identity

As part of a survey of the susceptibility of various lipids and mesophases to x-radiation damage, we examined qualitatively the effect that lipid headgroup, chain-to-glycerol linkage type, and mesophase identity have on the damage process (Fig. 8). To this end, a series of fully hydrated lipids, incubated at different temperatures so as to access the relevant mesophase, were exposed to x-radiation to the extent of ~15 Mrad in accumulated dose. Damage was evaluated as a noticeable change in the low-angle diffraction pattern, which starts out sharp and becomes less sharp, accompanied by an increase in diffuse scatter as damage of Type I sets in.

The results of this survey are shown in Table 1, where the severity of radiation damage is scored qualitatively. A perusal of the data in the table shows that the first two entries, DMPC and DPPC, succumb to Type I radiation damage in the $L_{\beta'}$ and L_α phases as described above. Both lipids are PCs with acyl chains in ester linkage to a glycerol backbone. None of the other entries in the table, which include ether-linked PC and ester- and ether-linked PEs in an assortment of phase states, including the lamellar crystalline (L_c), lamellar gel (L_β), $L_{\beta'}$, L_α, ripple ($P_{\beta'}$), and H_{II}, exhibit radiation damage as defined above. Parenthetically, we note that in the case of DHPE and 1,2-dimyristoyl-*sn*-glycero-3-phosphoethanolamine, a more extensive radiation exposure will eventually lead to Type II damage, as has been reported on previously for DHPE (Cheng et al., 1993).

The lipids included in this survey fall into two major groups: the diacyl-PCs on the one hand and the PEs and ether-linked PCs on the other. The former are profoundly sensitive to radiation damage, whereas the latter are considerably more resilient with their original mesophase, long-range order remaining intact up to relatively high dosage levels. Because our database is so limited, we will refrain from speculating on the origin of this disparate behavior.

TABLE 1 A qualitative evaluation of the effect of exposing fully hydrated ester- and ether-linked phospholipids to ~15 Mrad of 8-keV x rays*

Lipid	T (°C)	Mesophase	Damage effect‡
DMPC	10	$L_{\beta'}$	+
(Ester)	29	L_α	+/O
DPPC	30	$L_{\beta'}$	+
(Ester)	44, 65, 81	L_α	+
DHPC	4	$(L_{\beta I} + P_{\beta'})$§	−
(Ether)	44	L_α	−
DMPE	30, 44	L_c	−
(Ester)			
DPPE	30, 57	$L_{\beta'}$	−
(Ester)	67	L_α	−
DOPE	30	H_{II}	−
(Ester)			
DHPE	62	$L_{\beta'}$	−
(Ether)	72	L_α	−
	93	H_{II}	−

*For the lipid dispersion, 15 Mrad corresponds approximately to a 12-min exposure to 8-keV x rays at 2×10^{10} photons/s down a 0.3-mm collimator.
‡+ indicates substantial reduction in low-angle diffracted intensity amounting to $\tilde{A}_{002}$ (lamellar phases) and $\tilde{A}_{02}$ (H_{II} phase) values <0.5 at 15 Mrad. − indicates little or no change in the low-angle diffraction pattern ($\tilde{A}_{002}$ and $\tilde{A}_{02}$ >0.9 at 15 Mrad). +/O indicates limited reduction in low-angle diffracted intensity ($\tilde{A}_{002} \approx 0.8$ at 15 Mrad). See text for details.
§The diffraction pattern in this case suggests the coexistence of two phases as indicated. However, true phase identity was not determined in this study.

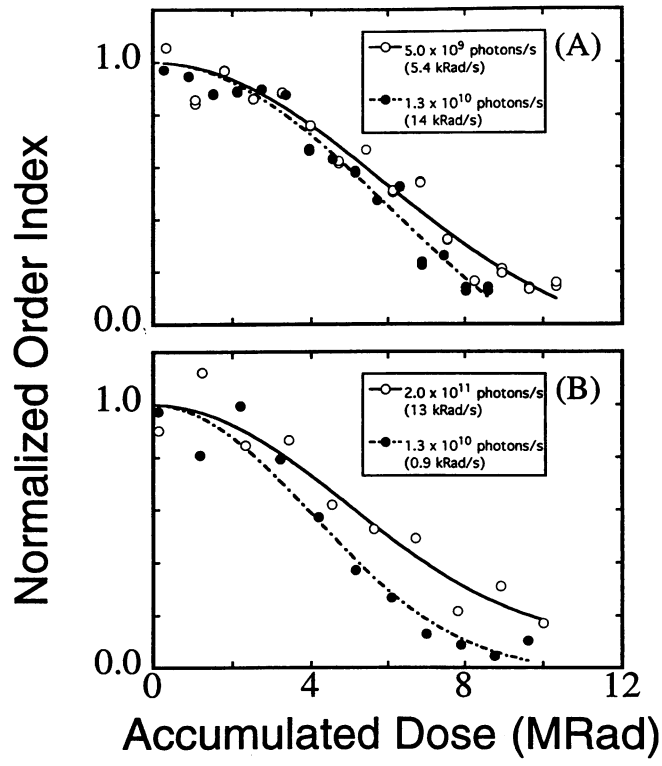

FIGURE 9 Effect of beam intensity on the susceptibility of fully hydrated DPPC dispersions (50% (w/w) water, $L_{\beta'}$ phase, 30.0°C) to x-radiation (8 keV) damage. Data in *A* and *B* were collected during different synchrotron experimental periods and from different sources and therefore should be compared with caution. The data in *A* were collected during a single experimental run at the A1 station at CHESS, and those in *B* were collected during a single experimental run at the X9A station at NSLS. See text for details.

However, we do note that the two groups identified above display distinctly different levels of order in their parent mesophase state. Thus, for example, the ester-linked PCs have lamellar reflections that are considerably broader and are accompanied by a higher level of diffuse low-angle scatter than is seen with the ether-linked PCs and the PEs (compare Fig. 3 and figure 1 in Cheng et al., 1993). It may be, therefore, that the lipids in the first group are intrinsically less well ordered to begin with and thus are more susceptible to the disordering effects brought on by the products of radiation damage.

Effects of x-ray intensity

Brighter, more intense x-ray sources are the wave of the future. Accordingly, the issue of beam intensity effects on radiation damage rate must be evaluated critically. It has been reported that crystals and solutions can better tolerate a fixed accumulated dose of x rays when the dose rate is higher (Helliwell, 1984; Raleigh et al., 1977; Stark, 1991, and references therein). This so-called inverse dose-rate effect has been rationalized in the context of radiation damage mediated by chain reactions involving free radicals (Stark, 1991).

Although the measurements made in the course of this study concerning beam intensity effects are not exhaustive, our data show no striking dose rate-dependence in the diffracted intensity variation observed with fully hydrated PCs (Fig. 9 *A*). The result obtained at the lowest dose rate used (0.9 krad/s) did show a small enhancement of damage compared to that seen at the higher rate (13 krad/s) for a given accumulated dose (Fig. 9 *B*). The range of dose rate variation examined, however, was limited to changing beam intensity by 15-fold. Obviously, further studies of this type are needed for a definitive conclusion concerning dose rate effects as applied to lipidic mesophases.

Miscellaneous factors

With a view to finding additives and experimental protocols that would not interfere with mesophase behavior and structure while reducing radiation sensitivity, we examined several likely candidates and strategies. These included 1) deoxygenation of the lipid dispersion, 2) addition to the dispersing medium of organic buffer compounds that might act as free radical scavengers, and 3) adjusting sample temperature.

Deoxygenation

Oxygen is known to be involved directly in lipid peroxidation (Stark, 1991). It has also been shown that $\cdot O_2^-$ can induce deesterification of lipids (Niehaus, 1978). We pos-

tulated therefore that removal of oxygen from the dispersion might help prevent, or at least lessen the severity of, radiation damage. To this end, a dispersion of DMPC was prepared in argon-saturated water (50% w/w) by mechanical mixing and was sealed in a quartz capillary in an argon atmosphere. Radiation sensitivity was evaluated by diffraction measurements at 29°C in the L_α phase as described above. In comparison with a control sample of DMPC prepared in air, the deoxygenated sample behaved no differently with regard to radiation damage. On the basis of this somewhat limited comparison, we conclude that deoxygenation has no apparent beneficial effect. However, we note that the lipid used contains myristoyl chains, which are saturated and are not particularly prone to peroxidation. A more extensive study of the effects of deoxygenation might involve the use of an unsaturated PC under fully hydrated conditions and in a phase where radiation damage develops rapidly.

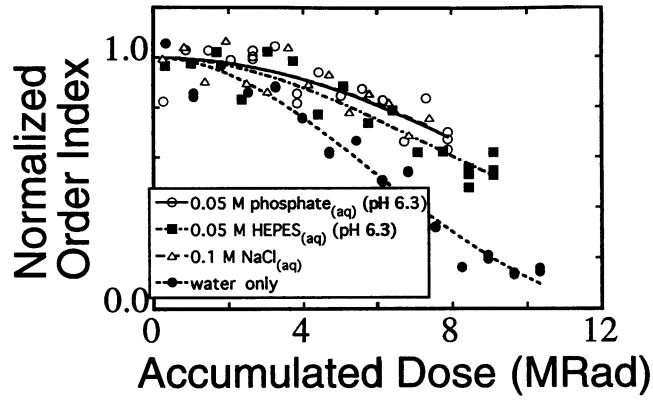

FIGURE 10 Effect of aqueous medium composition on the susceptibility of fully hydrated DPPC dispersions (50% (w/w) aqueous solution, $L_{\beta'}$ phase, 30.0°C) to x-radiation damage. The dispersing media used include 50 mM potassium phosphate buffer, pH 6.3; 50 mM HEPES/Cl buffer, pH 6.3; 0.1 M NaCl; and Milli-Q water.

Free radical scavengers

Free radicals derived from an organic substance dispersed in an aqueous medium can be generated either directly through the absorption of ionizing radiation by the organic compound itself or indirectly through reactions with nearby reactive free radicals produced as a result of water radiolysis (Stark, 1991). In this study, we focused on the water-derived radicals and sought to include in our system known radical scavengers used previously in water radiolysis studies. Important primary products of water radiolysis include 1) strong reducing agents such as the hydrated electron, e^-_{aq}, and the hydrogen atom, ·H; 2) strong oxidizing agents such as the hydroxyl radical, ·OH, and hydrogen peroxide, H_2O_2; and 3) the hydrogen molecule, H_2 (Stark, 1991). In the presence of oxygen, the superoxide anion radical, $\cdot O_2^-$, also plays an important role in effecting damage. Ethanol and formate are known ·OH scavengers (Raleigh et al., 1977). Buffer compounds such as HEPES and Tris have been shown to compete effectively with lipid for reaction with ·OH (Fiorentini et al., 1989). Naturally occurring antioxidants such as carotenoids, tocopherols, and ubiquinols also act as free radical scavengers (Ernster et al., 1992, and references therein). However, the problem in using many of these scavengers in combination with lipid is that they may alter mesophase behavior and thus complicate the system. Biological buffers are commonly used in model membrane studies and are relatively nonperturbing. They were examined in this study as potential radiation damage protectors.

DPPC, in an excess of the assorted buffer and salt solutions, was prepared by mechanical mixing as above, and its radiation sensitivity was monitored by x-ray diffraction in the $L_{\beta'}$ phase at 30°C. The results of the sensitivity study are presented in Fig. 10, where order index is plotted as a function of accumulated dose. Compared to a pure water control, the buffer and salt additives did give rise to a small attenuation in x-ray damage. However, the effect is small, and there are no obvious differences within the buffer series and between the buffer and the salt solutions. A more in-depth study of the effect of aqueous solutes on radiation damage is called for to determine whether the effects seen above are purely colligative.

Temperature

Temperature can influence radiation damage via its effect on radical reaction and diffusion rate. To test the effect of temperature on radiation sensitivity, a series of diffraction measurements were made using fully hydrated DPPC in the L_α phase at 44°C, 65°C, and 81°C (Table 1). During the

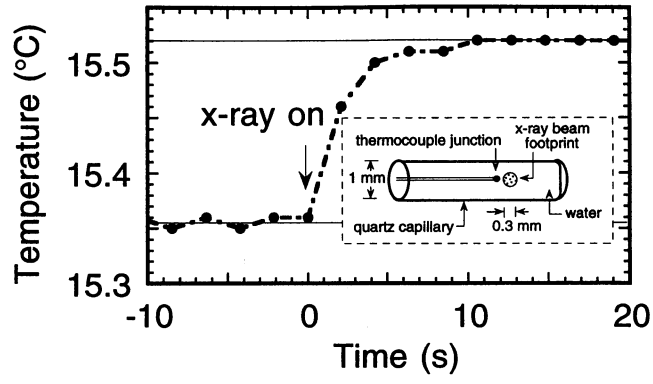

FIGURE 11 Heating effect of a 13.6-keV x-ray beam. Temperature rise was recorded by means of a T-type thermocouple junction (0.005-inch O.D. thermocouples; Omega Technologies Company, Stamford, CT) positioned in a 1-mm quartz capillary filled with Milli-Q water. The capillary was adjusted initially to position the junction directly in the x-ray beam. The capillary and thermocouple were then translated by 0.3 mm perpendicular to the x-ray beam along the length of the capillary so that the thermocouple was just to one side and within 0.3 mm of the x-ray beam (see inset). The temperature rise was recorded upon opening the beam shutter. Positioning of the thermocouple junction in the x-ray beam was facilitated by using a real-time x-ray area detector (Caffrey and Bilderback, 1983; Mencke and Caffrey, 1991) to monitor directly the shadow cast by the junction on diffuse x-ray scattering.

course of the exposure to 8-keV x rays up to an accumulated dose of ~15 Mrad, the deterioration in the diffraction pattern was remarkably similar at all three temperatures. These data suggest that radical diffusion and/or reaction rate must not be sufficiently sensitive to temperature in the limited range studied to elicit a noticeable effect on the development of radiation damage.

Sample heating by x rays

Sample heating by the incident x-ray beam is a natural consequence of a diffraction measurement. To quantify the effect, we measured the temperature change induced by exposure to an x-ray beam by placing a thermocouple in a 1-mm quartz capillary containing Milli-Q water, which was housed in a temperature-regulated sample holder. The thermocouple junction was carefully positioned to be within 0.3 mm of the interrogating x-ray beam. If we assume that the measured 8.6 krad of energy absorbed per second was used exclusively in sample heating (specific heat of water, 1 cal $g^{-1}°C^{-1}$), the calculated heating rate is ~0.02°C/s. Sample temperature will continue to rise with accumulated dose if adiabatic conditions prevail. The actual temperature rise will be limited, however, by heat transfer between the irradiated spot and the rest of the sample and the temperature-regulated sample holder. What we observed experimentally was that sample temperature increased rapidly (~0.05°C/s) at first and then reached a constant temperature some 0.16°C above ambient, presumably as a result of heat exchange (Fig. 11). Because the extent of sample heating is quite limited, it alone will not contribute significantly to the radiation damage process.

CONCLUSIONS

A quantitative evaluation of how x-ray damage to aqueous dispersions of phospholipids is affected by lipid chemical structure, mesophase identity, aqueous medium composition, and overall concentration, dose rate, and temperature is reported. X-ray diffraction, chromatography, and ESR measurements were used to monitor the damage process. In the course of this study, the following have been established: 1) In the case of diacyl-PCs, the apparent sensitivity to x-ray damage, as revealed by x-ray diffraction, is dependent on sample hydration. Thus, although the sample might have sustained significant damage as evidenced by TLC analysis, it is not obvious by diffraction under water-stressed conditions. An excess water phase is needed for the damage effects to be revealed. 2) Damage is profoundly sensitive to lipid identity, with the diacyl-PCs being most sensitive and the PEs and ether-linked PCs considerably less so. However, the effect seen is not particularly sensitive to mesophase type. 3) Organic buffers known to act as free radical scavengers had very little effect on the progress of damage above and beyond the effect seen with simple inorganic additives such as potassium phosphate and sodium chloride. 4) Deoxygenation was not effective in altering the course of radiation damage. 5) Adjusting temperature over a 36°C range had little effect on the development of damage symptoms. 6) Although limited in scope, our study of beam intensity effects did not show a pronounced inverse dose-rate effect. 7) Significant sample heating caused by the incident x-ray beam was detected. Despite the fact that the effect is small, it could create problems in studies where fine control over sample temperature is important. In this connection it is worthwhile noting that a small gradient in temperature will develop along the incident beam path in a sample as a result of absorption during the course of a diffraction or other such measurement. 8) Where damage is seen in the lamellar phases, it is accompanied by a disruption of the ordered multilamellar structure. This makes sense when viewed in the context of the breakdown products observed by TLC, which include free fatty acid and lysolipid. In a related study on PEs, we showed that damage leads to a loss of bilayered membrane structure and to the emergence of the inverted hexagonal phase (Cheng et al., 1993). ix) ESR measurements show that radiation damage is free radical mediated. Taken together, items viii and ix suggest a means by which free radicals, accumulating in cells during aging, will compromise membrane integrity and contribute to cell death.

This study serves to identify several key features that influence the outcome of measurements using high-flux x-ray sources. Because damage to sample structure and composition is a consequence of x-irradiation and is free radical mediated, these results have relevance in several areas and not just in the realm of problems related to using synchrotron x rays. However, it is the latter that inspired this study. Considering the import of x-ray methods as structure and spectroscopic probes and the current and projected use of extremely bright synchrotron sources, the problems of radiation damage must be duly recognized. The work reported on here represents a start in this increasingly important area. A lot more remains to be done, and time must be made available at synchrotron facilities worldwide to allow for a comprehensive evaluation and understanding of the problem, with a view to determining how it can be lessened or avoided completely.

We thank the entire CHESS (NSF, DMR12822) and MacCHESS (National Institutes of Health, RR-014646) staff and the X9B staff at NSLS (DOE, KP04-01 and -B043) for their help and support.

This work was supported by grants from National Institutes of Health (DK 36849 and DK 46295). A fellowship from Rohm and Haas Co. to AC is acknowledged.

REFERENCES

Blaurock, A. E. 1982. Evidence of bilayer structure and of membrane interactions from x-ray diffraction analysis. *Biochim. Biophys. Acta.* 650:167–207.

Briggs, J., and M. Caffrey. 1994. The temperature-composition phase diagram of monomyristolein in water: equilibrium and metastability aspects. *Biophys. J.* 66:573–587.

Caffrey, M. 1984. X-radiation damage of hydrated lecithin membranes detected by real-time x-ray diffraction using wiggler-enhanced synchrotron radiation as the ionizing radiation source. *Nucl. Instrum. Methods Phys. Res.* 222:329–338.

Caffrey, M. 1985. Kinetics and mechanism of the lamellar gel/lamellar liquid-crystal and lamellar/inverted hexagonal phase transition in phosphatidylethanolamine: a real-time x-ray diffraction study using synchrotron radiation. *Biochemistry.* 24:4826–4844.

Caffrey, M., and D. H. Bilderback. 1983. Real-time x-ray diffraction using synchrotron radiation: system characterization and applications. *Nucl. Instrum. Methods.* 208:495–510.

Caffrey, M., and D. H. Bilderback. 1984. Kinetics of the main phase transition of hydrated lecithin monitored by real-time x-ray diffraction. *Biophys. J.* 45:627–631.

Caffrey, M., and G. W. Feigenson. 1981. Fluorescence quenching of model membranes. 3. Relationship between calcium adenosinetriphosphatase enzyme activity and the affinity of the protein for phosphatidylcholines with different acyl chain characteristics. *Biochemistry.* 20:1949–1961.

Cevc, G., and D. M. Marsh. 1987. Phospholipid Bilayers. Physical Principles and Models. John Wiley and Sons, New York.

Cheng, A., J. L. Hogan, and M. Caffrey. 1993. X-rays destroy the lamellar structure of model membranes. *J. Mol. Biol.* 229:291–294.

Cheng, A., B. Hummel, A. Mencke, and M. Caffrey. 1994. Kinetics and mechanism of the barotropic lamellar gel/lamellar liquid crystal phase transition in fully hydrated dihexadecylphosphatidylethanolamine: a time-resolved x-ray diffraction study using pressure-jump. *Biophys. J.* 67:293–303.

Cheng, A., A. Mencke, and M. Caffrey. 1996. Manipulating mesophase behavior of hydrated DHPE: an x-ray diffraction study of temperature and pressure effects. *J. Phys. Chem.* 100:299–306.

Dittmer, J., and R. Lester. 1964. A simple, specific spray for the detection of phospholipids on thin-layer chromatogram. *J. Lipid Res.* 5:126–127.

Ernster, L., P. Forsmark, and K. Nordenbrand. 1992. The mode of action of lipid-soluble antioxidants in biological membranes: relationship between the effects of ubiquinol and vitamin E as inhibitors of lipid peroxidation in submitochondrial particles. *BioFactors.* 3:241–248.

Evans, C. A. 1979. Spin trapping. *Aldrichimica Acta.* 12:23–29.

Fiorentini, D., L. Landi, V. Barzanti, and L. Cabrini. 1989. Buffers can modulate the effect of sonication on egg lecithin liposomes. *Free Radic. Res. Commun.* 6:243–250.

Helliwell, J. R. 1984. Synchrotron x-radiation protein crystallography: instrumentation, methods and applications. *Rep. Prog. Phys.* 47: 1403–1497.

Hui, S. W. 1980. Radiation damage of phosphatidylcholine bilayers: effects of temperature and hydration. *Ultramicroscopy.* 5:505–512.

Janiak, M. J., D. M. Small, and G. G. Shipley. 1976. Nature of the thermal pretransition of synthetic phospholipids: dimyristoyl- and dipalmitoyllecthin. *Biochemistry.* 15:4575–4580.

Janiak, M. J., D. M. Small, and G. G. Shipley. 1979. Temperature and compositional dependence of the structure of hydrated dimyristoyl lecithin. *J. Biol. Chem.* 254:6068–6078.

Jansson, M., R. Thurmond, T. Trouard, and M. Brown. 1990. Magnetic alignment and orientational order of dipalmitoylphosphatidylcholine bilayers containing palmitoyllysophosphatidylcholine. *Chem. Phys. Lipids.* 54:157–170.

Katsaras, J., R. Stinson, E. J. Kendall, and B. D. McKersie. 1986. Structural simulation of free radical damage in a model membrane system: a small-angle x-ray diffraction study. *Biochim. Biophys. Acta.* 861: 243–250.

MacGillavry, C. H., and G. Rieck. 1983. International Tables for X-ray Crystallography. D. Reidel Publishing, Boston.

Makino, K., N. Suzuki, F. Moriya, S. Rokushika, and H. Hatano. 1981. A fundamental study on aqueous solutions of 2-methyl-2-nitrosopropane as a spin trap. *Radiat. Res.* 86:294–310.

Mariani, P., and F. Rustichelli. 1989. Structural modifications induced by external agents on multilamellar liposomes. *Prog. Microemulsions.* 41: 251–261.

Mencke, A. P., and M. Caffrey. 1991. Kinetics and mechanism of the pressure-induced lamellar order/disorder transition in phosphatidylethanolamine: a time-resolved x-ray diffraction study. *Biochemistry.* 30:2453–2463.

Niehaus, W. G. J. 1978. A proposed role of superoxide anion as a biological nucleophile in the deesterification of phospholipids. *Bioorg. Chem.* 7:77–84.

Raleigh, J. A., W. Kremers, and B. Gaboury. 1977. Dose-rate and oxygen effects in models of lipid membranes:linoleic acid. *Int. J. Radiat. Biol.* 31:203–213.

Stark, G. 1991. The effect of ionizing radiation on lipid membranes. *Biochim. Biophys. Acta.* 1071:103–122.

Stout, G. H., and L. H. Jensen. 1989. X-ray Structure Determination—A Practical Guide. John Wiley and Sons, New York.

Swartz, H. M., and S. M. Swartz. 1983. Biochemical and biophysical applications of electron spin resonance. *Methods Biochem. Anal.* 29: 207–323.

Wiener, M. C., and S. H. White. 1991. Fluid bilayer structure determination by combined use of x-ray and neutron diffraction. *Biophys. J.* 59:162–173.